Subduction of the Rivera plate beneath the Jalisco block as imaged by magnetotelluric data

Fernando Corbo-Camargo[1*], Jorge Arturo Arzate-Flores[2], Román Álvarez-Béjar[3], José Jorge Aranda-Gómez[2], and Vsevolod Yutsis[4]

[1]Posgrado en Ciencias de la Tierra, Centro de Geociencias, Universidad Nacional Autónoma de México, Blvd. Juriquilla no. 3001, C.P. 76230, Querétaro, Mexico.
[2]Centro de Geociencias, Universidad Nacional Autónoma de México, Blvd. Juriquilla no. 3001, C.P. 76230, Querétaro, México.
[3]Instituto de Investigaciones en Matemáticas Aplicadas y en Sistemas (IIMAS), Universidad Nacional Autónoma de México, Circuito Escolar, C.P. 04510, Ciudad Universitaria, México D.F., Mexico.
[4]Facultad de Ciencias de la Tierra, Universidad Autónoma de Nuevo León, Carretera a Cerro Prieto Km. 8, Ex Hacienda de Guadalupe, C.P. 67700, Linares N.L., Mexico.
** fercorbo@gmail.com*

ABSTRACT

Two magnetotelluric (MT) profiles perpendicular to the trench provide information on the subduction of the Rivera plate under the Jalisco block (JB). The geometry of the subducting slab is inferred by the anomalous conductor on the top of the profile in the central part of the JB. High conductivity zones (<50 ohm-m) at depths shallower than 10 km are associated to dewatering of the oceanic crust below the accretion prism in the SW of the profile. Away from the coast, observed upper crustal conductors (<10 km) are interpreted as partial melt related to the Central Jalisco volcanic lineament. The source of the crustal conductor in the central part of the MT profile, ~25–75 km inland and depths between 40 and 60 km, is interpreted as a region of interconnected fluids associated with the metamorphic dehydration of the oceanic plate. Contrasting resistivity in the mantle wedge at depths below 40 km suggests that hot mantle material may be migrating upwards, mixing with dehydration reaction products. Near Bahía de Banderas subduction appears steeper closer to the trench than toward the SW suggesting a twisted oceanic subducting slab beneath the continental crustal block. Our results support the mantle upwelling model as an explanation for the reported 1.5 km uplift of the central part of the JB and subsidence of the fore arc region, as well as a change in mantle properties at the NW edge of the JB, which is backed by seismic data.

Key words: magnetotelluric images, subducting slab, mantle upwelling, Jalisco block, Mexico.

RESUMEN

Dos perfiles magnetotelúricos (MT) perpendiculares a la trinchera proporcionan información del proceso de subducción de la placa de Rivera debajo del bloque de Jalisco (BJ). A partir del conductor anómalo inclinado que se asocia a la interface activa se deducen rasgos de la geometría de la placa que subduce. Zonas de conductividad anómala (<50 ohm-m) a profundidades inferiores a los 10 km se asocian a la deshidratación de la corteza oceánica debajo del prisma de acreción en el SW del perfil. Lejos de la costa, los conductores observados a profundidades de la corteza superior (<10 km) se

Corbo-Camargo, F., Arzate-Flores, J.A., Alvarez-Béjar, R., Aranda-Gómez, J.J., Yutsis V., 2013, Subduction of the Rivera plate beneath the Jalisco block as imaged by a magnetotelluric data: Revista Mexicana de Ciencias Geológicas, v. 30, núm. 2, p. 268-281.

interpretan como zonas de fusión parcial relacionadas al lineamiento volcánico de Jalisco Central. La fuente de la zona conductora cortical en la parte central del perfil MT, aproximadamente 25 a 75 km dentro del continente y entre los 40 y 60 km de profundidad, se interpreta como una región de fluidos interconectados asociados con la deshidratación de la corteza oceánica por procesos de metamorfismo. El contraste de resistividades en la cuña del manto debajo de ~40 km sugiere la migración ascendente de material caliente del manto que se mezcla con productos de reacciones metamórficas de la placa oceánica. El proceso de subducción de la placa de Rivera ocurre a un ángulo más pronunciado y más cercano a la trinchera en la parte noroeste que hacia la parte sureste de la zona de subducción, lo que sugiere una placa oceánica flexionada hacia el NW debajo del bloque de corteza continental. Nuestros resultados apoyan un modelo de ascenso del manto en la parte centro oriental del BJ, que explica el levantamiento topográfico de más de 1.5 km y la subsidencia en la zona del ante-arco reportada, además de un cambio en las propiedades eléctricas del manto en la zona, que parecen variar rápidamente, como lo sugieren también los datos sísmicos.

Palabras clave: perfiles magnetolelúricos, placa en subducción, ascenso del manto, bloque Jalisco, México.

INTRODUCTION

The Jalisco block (JB) is a portion of the complex convergent plate boundary involving the subduction of the Rivera and Cocos oceanic plates beneath the North American continental crust. Its evolution includes rifting, batholith intrusion, early Cretaceous to Holocene volcanism, and active sedimentation (Taran *et al.*, 2002). It is located between 19 and 21 degrees of latitude north, and 104 and 106 degrees of longitude west. The inland limits of the JB (Figure 1) are two rift systems, namely the Colima and the Tepic-Zacoalco extensional zones located east and north of the JB, respectively (Allan *et al.*, 1991; Ferrari, 1995; Rosas-Elguera *et al.*, 1996; Álvarez, 2002; Taran *et al.*, 2002). The offshore limits are more ambiguous, although the Barra de Navidad fault (Figure 1a), and the submarine portion of the Manzanillo graben (Bourgois *et al.*, 1988) have been proposed as part of these limits.

The JB can be divided into two domains based on the lithology of the exposed rocks. These are referred to as the southwestern and northeastern domains (Maillol *et al.,* 1997*;* Alvarez *et al.*, 2006). Outcrops in the southwestern domain are mainly Cretaceous to Paleocene calc-alkaline intrusive rocks (granite to tonalite, 100 to 60 Ma: Schaaf *et al.*, 1995) and Cretaceous sedimentary and volcanosedimentary roof pendants (Figure 2). The Puerto Vallarta batholith is a high-silica granite with occasional white mica. Plagiogranites, gabbros, granites and granodiorites occur at the Manzanillo pluton. Late Triassic metasedimentary rocks and Middle Jurassic (~130 Ma) marine turbidites, outcropping in small areas, are similar to those found in the Guerrero and Alisitos terranes (Schaaf *et al.*, 1995).

The northeastern domain is bounded by the Tepic-Zacoalco rift to the NE and the northern and central parts of the Colima rift to the SE (Figure 1). Most of the exposed rocks are volcanic and range in age from Cretaceous (114 Ma: Ferrari *et al.*, 2000) to Pleistocene. Early Pliocene and Quaternary volcanoes form four volcanic fields: San Sebastián, Mascota, Los Volcanes-Atenguillo, and Ayutla (ellipses in Figure 2). A narrow zone connecting the southern ends of these fields form the NW-trending Central Jalisco volcanic lineament (CJVL). Isotopic ages for the CJVL obtained by Bandy *et al.* (2001) suggest younger volcanism towards the northwest of the JB. Composition of the volcanic rocks correspond to the three different magma series recognized in the Trans-Mexican Volcanic Belt: alkaline-potassic (lamprophyre), calc-alkaline, and intraplate alkaline (Gómez-Tuena *et al.*, 2007). A remarkable feature of the JB is that most of the "true lamprophyres" analyzed in Mexico come from the CJVL and from the nearby Colima rift (Luhr *et al.*, 2006). Lamprophyres are coeval with calc-alkaline volcanic rocks throughout the CJVL (Luhr *et al*., 2006; Righter and Rosas-Elguera, 2001). Within the JB, only the northern part of the Los Volcanes-Atenguillo volcanic field is formed by alkaline/high Nb intraplate-type volcanic rocks (Righter and Carmichael, 1992). Rock composition in the whole CJVL, in terms of silica content, ranges from ~48.5 wt% – 56 wt% and most rocks contain nepheline in the CIPW norm (Luhr, 1997). The magmatic diversity of western Mexico has been explained by invoking contributions of chemically different subduction agents as a function of slab depth and residual mineralogy: a low-pressure/temperature aqueous fluid would induce melting of the peridotitic mantle wedge and form typical calc-alkaline volcanoes, whereas a deeper and hotter slab-derived melt (or supercritical liquid) would contribute to the formation of potassic magmas due to phengite/monazite/allanite breakdown. In this context, intraplate-like magmas derive from decompression melting of the upper mantle as a natural consequence of subduction geodynamics (Gomez-Tuena *et. al.*, 2011).

The limit between the southwestern and northeastern domains coincides with a drainage divide located at the Cacoma and Manantlán ranges (Figure 2b). The Talpa and Mascota rivers flow northwestward until they reach the Valle de Banderas graben (Figure 1), where they turn towards the southwest (Figure 2b). The Armería river drains the eastern

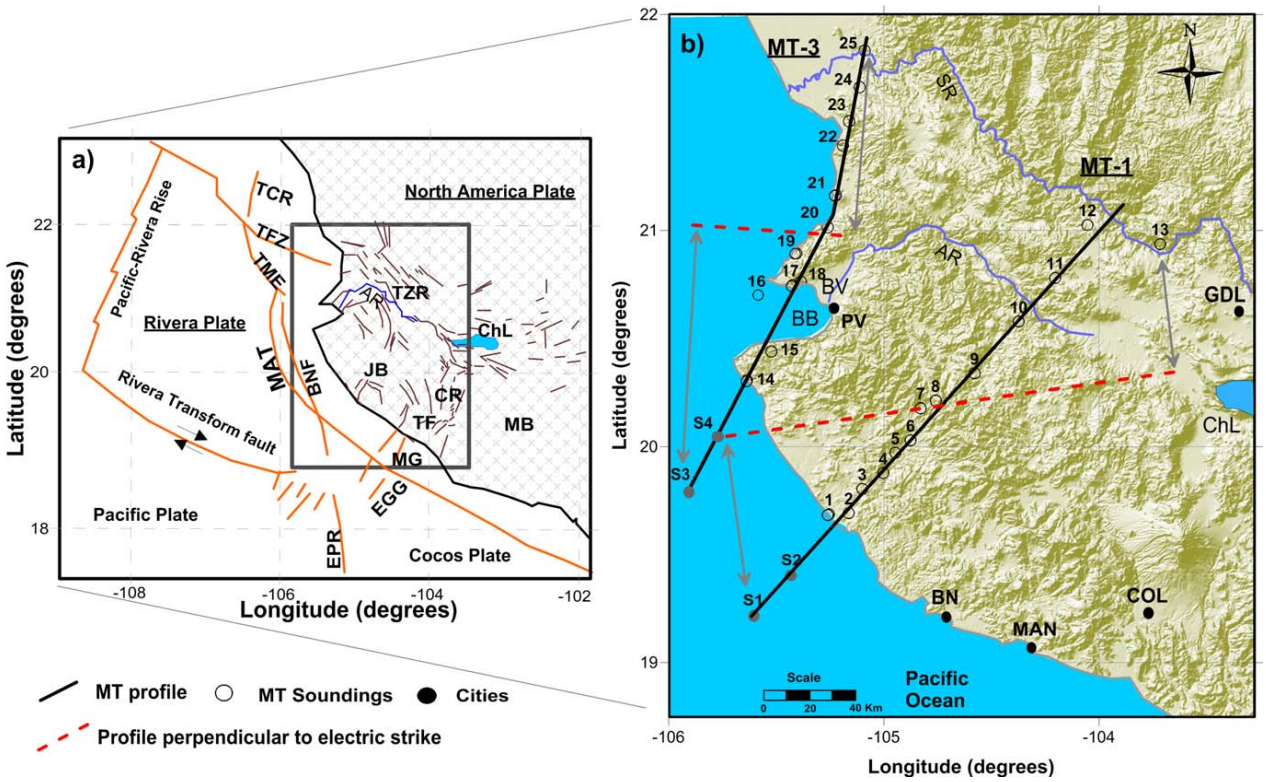

Figure 1. a: General tectonic setting of the Jalisco block area compiled from Allan (1986), Luhr *et al.* (1985), Bourgois *et al*. (1988), and Ferrari *et al.* (1994). The Tepic-Zacoalco rift zone (TZR) and the Colima rift (CR) are regarded as the northern and eastern inland limits of the Jalisco block (JB) respectively. A NW limit has been proposed along Bahía de Banderas (BB) and Valle de Banderas (BV) and its continuation to the TZR (Johnson and Harrison 1990; Alvarez, 2002). Offshore limits are the Middle America trench (MAT) to the NW, whereas the Manzanillo Graben (MG) could be the southern continuation of the Colima rift towards the Middle America trench (MAT). The Tamazula fault has been also proposed as the SE limit of the JB (Garduño-Monroy *et al*., 1998). Other abbreviations: TCR: Tamayo Canyon rift; EPR: East Pacific Rise; ChL: Chapala lake; TFZ: Tamayo fault zone; EGG: El Gordo graben; TME: Tres Marías escarpment; MB: Michoacán block; TF: Tamazula fault; BNF: Barra de Navidad fault. b: location of the MT stations and interpreted profiles (black lines) are shown. Dashed red lines indicate the ideal profile orientation for 2D inversion. AR: Ameca river; SR: Santiago river; PV: Puerto Vallarta; COL: Colima; GDL: Guadalajara; MAN: Manzanillo; BN: Barra de Navidad.

half of the northeastern domain, and flows southeastward until it reaches the area located south of the Colima volcanic complex (Figure 2b). Clearly, the CJVL is located immediately northeast of a highland which runs parallel to the Pacific coast and the portion of the Middle America trench (MAT) between Bahía de Banderas and Manzanillo (Figure 2b).

Two of the most remarkable features of the JB are the belt of calc-alkaline batholiths exposed from Puerto Vallarta to the Colima rift, and the late Cretaceous (85–74 Ma) and Eocene (56–48 Ma) uplift of the southeastern domain of the block. Both phenomena are attributed to continental margin truncation caused by tectonic erosion during periods of high convergence rate, one at the beginning of the Eocene (54–50 Ma) and other that began at the early Oligocene (33 Ma) (Calmus *et al.,*1995). In addition, Durham *et al.* (1981) provided evidence of post-Miocene (<5 Ma) uplift (>0.06 mm/a) along the JB coast, based on geological and paleontological data, and Ramírez-Herrera *et al.* (2004) inferred an average uplift of 3 mm/a of the JB during the last 1300 years using radiocarbon dates of emergent paleoshorelines along the coast. Finally, a Neogene subsidence event has been reported by Mercier de Lépinay *et al.* (1997) in the offshore area off Manzanillo where the authors estimated an average subsidence rate of 0.35 mm/yr, which provides indirect proof of active tectonic uplift of the JB.

The present study aims at interpreting the observed electrical structure beneath the JB to deliver clues on the mechanism behind the uplift process. This is attempted through a magnetotelluric study in the central portion of the JB arranged as profiles perpendicular to the trench. The results reveal the main crustal features at depths of ~60–70 km, in a region where seismic tomography has low resolution (Yang *et al.*, 2009). This makes the higher-resolution magnetotelluric models of particular interest.

THE SUBDUCTION OF THE RIVERA AND COCOS PLATES

Subduction was continuous from Alaska to South America before the Middle Oligocene; in the Middle Miocene, the Baja California peninsula began separating

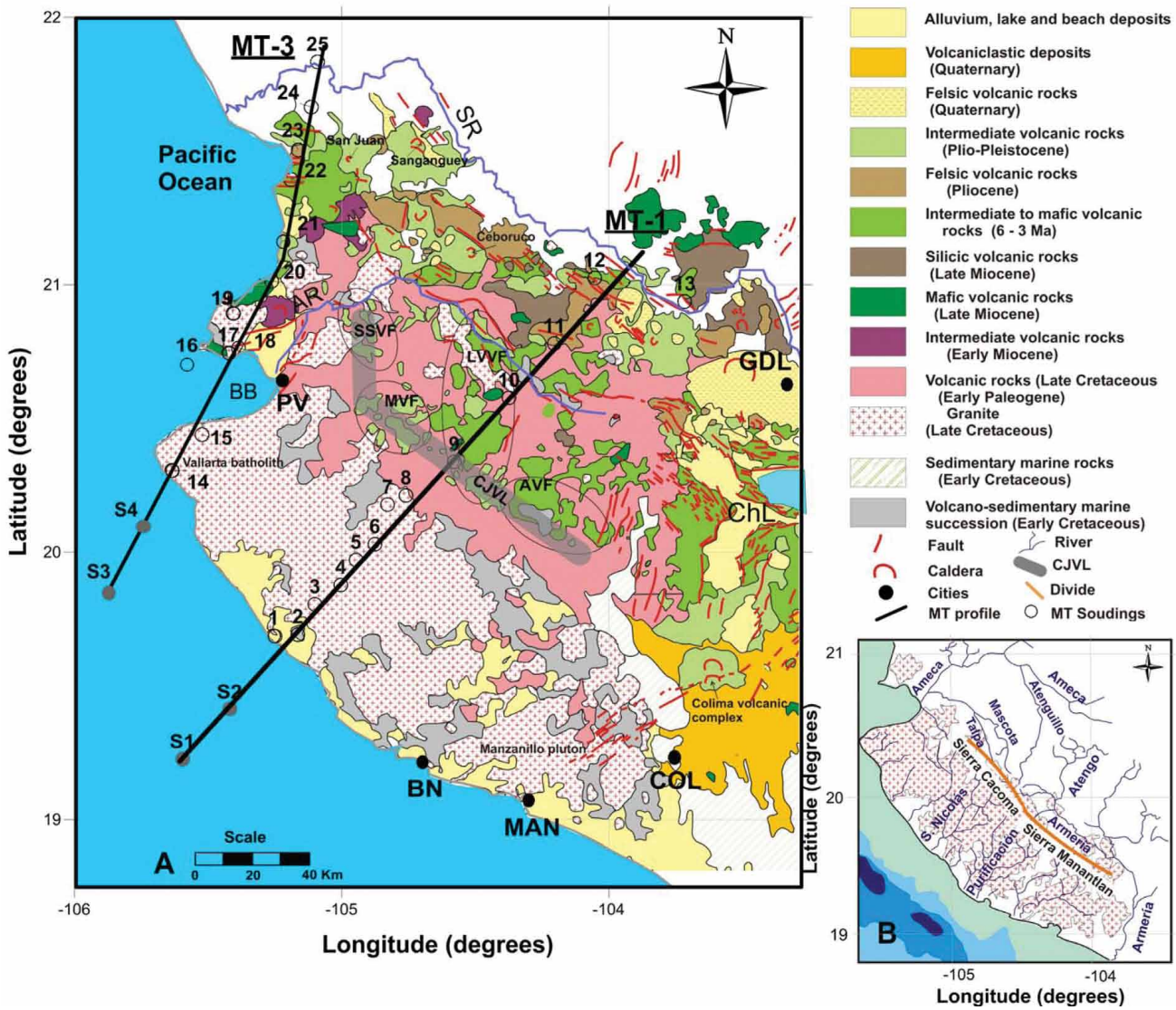

Figure 2. a: Geologic map of the Jalisco block modified from Servicio Geológico Mexicano (2007) and Gómez-Tuena *et al.* (2007), showing the subsided (SW) and uplifted (NE) domains mentioned in the text. Outcrops near the coast are dominated by Mesozoic calc-alkaline intrusive rocks and roof pendants composed by metasedimentary and volcanosedimentary sequences. The pre-Cenozoic succession is dominated by silicic ash-flow tuffs of Cretaceous age (Righter and Rosas-Elguera, 2001) in the northeastern sector, where there is an extensive cover of late Cenozoic volcanic rocks. The Central Jalisco volcanic lineament (CJVL), composed by the San Sebastián (SSVF), Mascota (MVF), Los Volcanes (LVVF), and Ayutla (AVF) volcanic fields, together with the Colima volcanic complex, represents the magmatic front in the region. The two MT profiles and sites numbers are also shown. b: The simplified drainage pattern defines the hydrologic divide of the JB (orange line in b) along the sierras Cacoma and Manantlán, which coincides with the limit between the lithologic domains. Other abbreviations as in Figure 1.

from mainland Mexico (Atwater and Stock, 1998). A single plate subducting along a unique trench up to that time would be expected. However, such behavior was modified since the initial separation stages of the peninsula from mainland Mexico at ~14 Ma. At about that time the Magdalena microplate subducted under Baja California and the Jalisco block when they were still coupled together. At around 11 Ma the Rivera plate separated from the Cocos plate (DeMets and Traylen, 2000). The Pacific-Rivera spreading center initially extended as far south as the Clipperton fracture zone (Klitgord and Mammerickx, 1982), however, as the Mathematician ridge was abandoned the boundary between the plates was successively displaced northward, diminishing the original area of the Rivera plate. During the dynamic processes not only Baja California was rifted away, but the previously continuous trench was segmented and separated. Subduction along the peninsula ceased gradually, however, south of the JB the Cocos plate continued subducting.

Bandy *et al.* (1995) postulated that the limit between the Rivera and Cocos plates runs from El Gordo graben (EGG) and continues at depth along a line located east of

the Colima rift (Figure 1). However, Garduño-Monroy *et al*. (1998) sustain that the SE limit of the JB is the Tamazula fault. On the other hand, recent seismic tomography (Yang *et al.*, 2009) revealed that while there is no divergence at the trench between the motion of the two plates, there is a gap at depth between the two plates under the Colima rift. According to Yang *et al.* (2009), the gap may have caused a toroidal mantle flow favoring slab rollback and a steeper dip angle beneath the JB. The Rivera plate seismicity is not only lower than at the Cocos plate, but it is also shallower and ends in a seismic gap between latitudes of 19.5º and 20.5º (Núñez-Cornú *et al.*, 2002), which provides seismic evidences that the subducting slab shallows towards the NW. Another seismic study at the northern terminus of the MAT (Brown, 2007) shows that the oceanic crust underplates the continental crust north of Bahía de Banderas at depths of 30 km to its top, at a distance of 135 km from the trench.

MAGNETOTELLURIC SURVEY

Magnetotelluric (MT) surveys have been extensively used to probe plate convergent margins in many parts of the world. There are examples of the utility of the method to study physical processes beneath tectonically active zones. This is particularly true for the American continent along the eastern Pacific margin, for which a large number of MT studies with this purpose have been conducted (*e.g.*, Kurtz *et al.*, 1986, 1990; Waff *et al.*, 1988; Wannamaker *et al.*, 1989; Schwarz and Kruger, 1997; Arzate *et al*., 1995; Jording *et al*., 2000; Brasse *et al.*, 2002; Jödicke *et al.*, 2006; Soyer and Unsworth, 2006; Brasse *et al*, 2008). Subduction related anomalous conductors have been associated to the presence of fluids in the lower crust in this type of environment. Hyndman (1988) observed that interconnected, slightly saline (~0.5 –3%) water would be sufficient to reproduce the enhanced conductivities observed in the continental crust associated to the subduction of the oceanic lithosphere. The dehydration of the oceanic plate in terms of metamorphic reactions is presumed to occur on top of the slab at different T-P conditions and is invoked to explain the observed widespread enhanced conductivities associated to petrological differentiation or partial melting during subduction (Jödicke *et al*., 2006).

The magnetotelluric survey was conducted within the Jalisco Block; profile MT-1 extends from the SW coast of northern Jalisco across the boundary between the coastal region and the uplifted domain of the JB (Alvarez *et al*., 2006) reaching the NW-SE Tepic-Zacoalco rift zone; and profile MT-3 runs from the westernmost point of the JB, aligned with the Marieta island (Site 16) and along the western edge of the JB. Figures 1 and 2 show the location of the MT profiles, which are roughly perpendicular to the trench. The profiles comprise 25 stations with variable separation (~5 to 20 km), both starting at the shoreline and extending ~200 km in a N-NE direction. We acquired the data at each site registering continuously during periods of 22–24 hours using two MTU-2000 Phoenix magnetotelluric systems and measuring in the frequency range of 10^{2} to 10^{-3} Hz. The acquired time series of the measured electromagnetic (EM) fields (*ex, ey, hx, hx, hz*) were processed using standard fast fourier transform (FFT; *e.g.*, Simpson and Bahr, 2005) and robust cascade decimation (Wight and Bostick, 1980) algorithms. The resulting impedances were then converted to resistivities and phase shift field curves that provided the basis of the resulting electrical model.

Induction vectors, geoelectric strike

Deviations of the 2D case are indication of geological complexity, which could be interpreted in terms of the regional geology. There are a variety of methods to test the dimensionality of the ground from the MT impedance tensor complex elements (*e.g.*, Swift, 1967; Bahr, 1988, 1991; Groom and Bailey, 1989; Weaver *et al.*, 2000; Caldwell *et al.*, 2004; Martí *et al.*, 2004); however, some are more stable for noisy data, although probably less sensitive to structural changes. We tested several methods and found that the phase-based distortion tensor of Caldwell *et al.* (2004) provides more stable and consistent dimensionality results, and the 2D/3D superposition model of Bahr (1988) for the regional strike estimations. In Figure 3 we present in plan view the tensor phase ellipses obtained along the MT profiles, which show a predominantly N-NW electric strike direction for MT-1 and N-NE for MT-3. This suggests a mostly two-dimensional conductivity structure but with regional variations, as suggested by a distinctive split of about 10 degrees between the higher (100–1 Hz) and lower (1–0.01 Hz) frequency ranges and by the average of deflected induction vectors in this zone (Figure 3). The weighted average strike angle obtained from the data for profile MT-1 was θ = N9W and for profile MT-3 was θ = N5E (marked with yellow lines in Figure 3b). General orientation of the ellipses associated to the electric strike of the region are consistent with main faulting directions of the Talpa, Mascota, and Atenguillo grabens in the central and NW parts of the JB. This suggests that the electrical strike azimuth in this zone is closely related to structural lineaments that prevail at lower crustal depths, probably related to the direction of the anisotropic mantle in the zone (León-Soto *et al.*, 2009), and roughly coinciding with the Rivera plate motion direction (*e.g.*, Yang *et al.*, 2009). However, there are significant spatial variations of strike directions in some areas of the MT survey that are indicative of structural differences associated to changes in the tectonic regime in the surroundings of the JB. The dispersion of the regional electric strike, often affected by large faults and other conductive structures, occur particularly at the northern limit of the JB, within the Tepic-Zacoalco extensional zone, and across the Bahía de Banderas fault zone. The induction vectors, plotted using the Parkinson convention (Figure 3)

and obtained from the measured vertical field component for the complete frequency range and for all sites, yield a quite consistent orthogonal direction for MT-1 but shows an important discrepancy for profile MT-3. At least part of this behavior may be attributed to the proximity of the sea; however, the thin water layer (~100 m) of the shallow platform is unlikely to be affecting the low frequency range of our data, for that the observed distortion of the induction vectors at frequencies below ~1 Hz is assumed to be related to crustal structure. We regard the scattering of the induction vectors azimuth of profile MT-3 as evidence of the structural complexity in the northwestern limit of the JB, partly due to the proximity of the Bahía de Banderas fault zone (Arzate *et al*., 2006). The dimensionality analysis of the data suggests that at least for a frequency band above 0.01 Hz the ground can be considered as two-dimensional along the modeled MT-1 profile, except for sites 12 and 13 for which the frequency band is reduced (above 0.1 Hz). Even though, the mostly two-dimensional behavior of the data at frequencies above 0.01 Hz, indicates that the conductivity structure can be modeled based on a 2D inversion scheme.

2D INVERSION OF MT DATA

All sites of profile MT-1 were rotated to the regional strike (θ = N9W) and projected onto a profile line of azimuth N81E (dashed line in Figure 1) in order to meaningfully apply a 2D inversion algorithm. For the inversion of profile MT-3 we followed a similar strategy as for the MT-1; all sites were rotated to the corresponding regional electrical strike azimuth (θ = N5E) and a joint 2D inversion (transverse electric or TE, transverse magnetic or TM, and tipper) was performed using Rodi and Mackie (2001) inversion algorithm with same initial conditions: a 100 columns-50 rows mesh and 100 ohm-m half space model, as well as

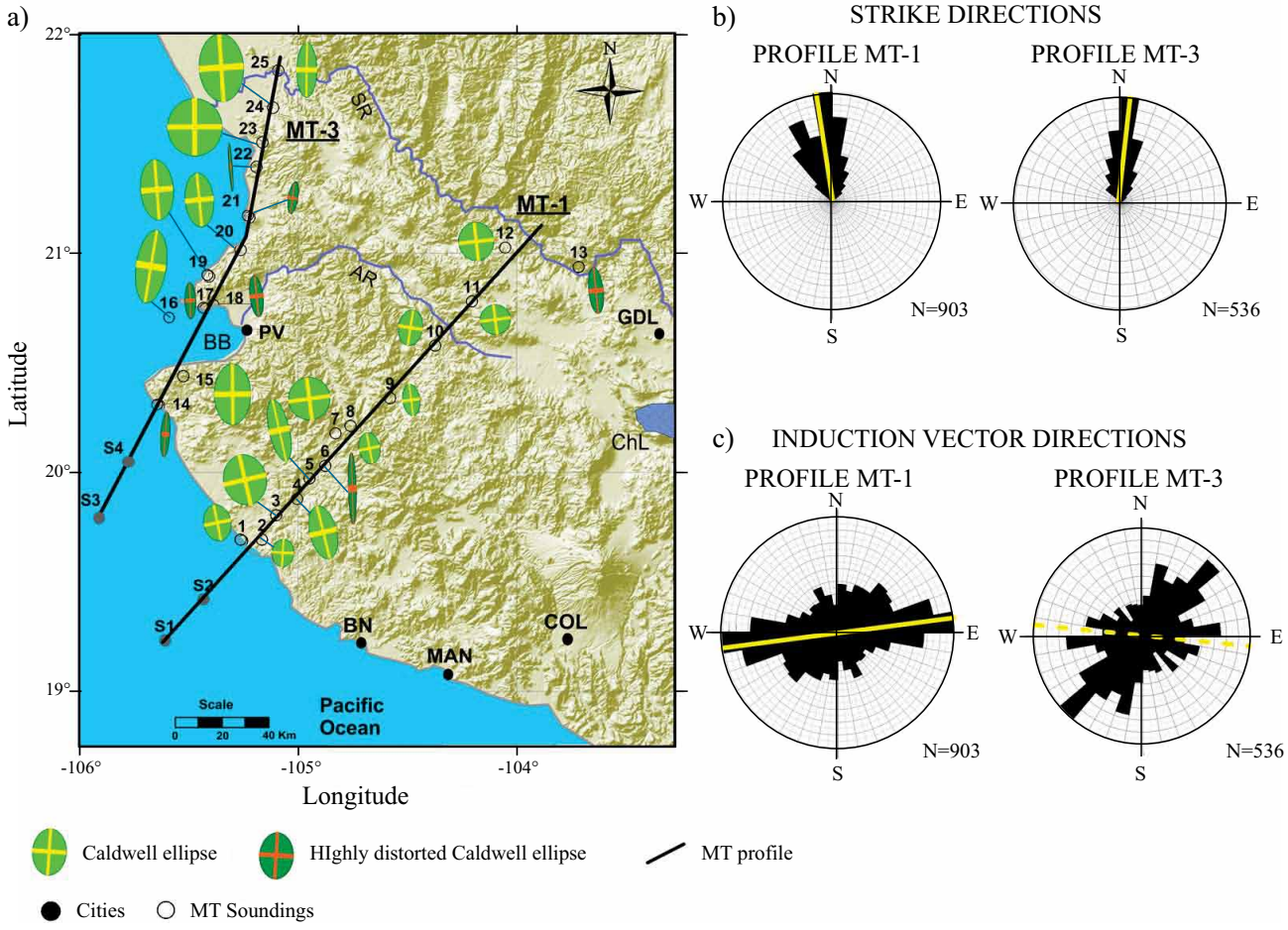

Figure 3. a: Phase tensor ellipses (Caldwell *et al*., 2004) along the MT transects (left side) indicating the electrical strike along the major axis. The regional electrical strike (Bahr, 1988, 1991) corresponds to the main regional conductive structure comparable with faulting directions in central and northwestern parts of the Jalisco block. Both, the electrical strike azimuth and phase tensor ellipses are roughly coincident with share wave fast direction of polarization within the mantle (León-Soto *et al*., 2009) related to the direction of the main stress field. The average strike for profile MT-1 yields an azimuthal angle of θ = N9W and for MT-3 of θ = N5E (yellow line in b). The induction vectors (c) were obtained from the vertical magnetic field, and produce consistent orthogonal direction for profile MT-1, which provides independent evidence of a consistent 2D earth in this part of the survey area. However, induction vectors azimuth for MT-3 are inconsistent with the strike azimuth, which implies structural complexity in the NW limit of the Jalisco Block.

same error floors. The best sites average root mean square (RMS) misfit obtained for both MT-1 and MT-3 was below 4.7% after 65 minimum iterations. To take into account the sea effect we have included two offshore synthetic soundings in each inverted profile, namely S1, S2 for MT-1 and S3, S4 for MT-3. The oceanic layer thicknesses were taken from bathymetric data at the four locations, and the oceanic crustal thickness used was 7500 m for all synthetic sites. The water layer and slab resistivities were 0.2 ohm-m and 1000 ohm-m, respectively, which are accepted values for such media (*e.g.*, Simpson and Bahr, 2005). The joint 2D inversion was carried out using a half space starting resistivity of 100 ohm-m, including the constrictions imposed by the fix synthetic resistivity structure offshore. We have done a number of test inversions varying the grid size, and always obtained the same main conductive features in the final models.

The fitting data strategy consisted in inverting the phases first by allocating large error floors to resistivities (>50%) and keeping low error floors for the phases (<5%). Subsequently, both error floors were kept low, 10% for resistivities and 5% or less for phases, until RMS average values for the sites were lower than 5%. Figure 4 shows the fitting curves for profile MT-1 with the best misfit (RMS= 4.7) obtained after 65 iterations. Static shift of data curves were minimum between sites and, when present, curves were corrected to resistivity levels of nearby sites. Applied corrections were generally smaller than one order of magnitude. We chose to minimize second derivatives using uniform Laplacian and a smoothing factor (τ) of 4. This value was determined through the optimization of the tradeoff between the RMS misfit and the smoothing of the models. The results for profile MT-1 are shown in Figure 5. In order to evaluate the influence of the conductors in the final result, the three main conductive zones were removed consecutively from the model. For each zone, a forward model was run replacing the respective conductor by a fixed background resistivity of 2000 ohm-m. This was done successively, first replacing the Zone 1 (conductors A, B and C), then the Zone 2 (conductors D, E and F), and finally the Zone 3 (conductor H). The RMS error increases considerably when the conductors are removed (Figure 5a) thus revealing that their presence is required by the data. The penetration depth of the EM signal was estimated at all MT sites by applying the Niblett-Bostick approximation that uses the average conductance for a layered earth (Niblett and Sayn-Wittgenstein, 1960; Bostick, 1977). Vertical grey lines in the resistivity section (Figure 5b) are the estimated depths of investigation obtained using the TE mode, which in general yields underestimated depth values with respect to those obtained using the TM mode of polarization (Jones, 1983). This suggests that penetration depths, which are in fact lower limits of investigation, are enough to probe the observed electrical conductivity structure down to depths of 60 km, and in some cases down to 80 km. For comparison, we also inverted the profile with the sites rotated to the principal axis (variable strike with frequency) using the same inversion parameters and mesh described above. The resistivity image obtained from the N9W rotated and projected model (a), the inverted polarity (b), and the rotated to the principal axis model (c) for profile MT-1 are shown in Figure 6. Observed differences between the principal axis and the regional strike models are mainly in the SW half of the profile, where most of the upper crustal anomalous conductors lie. However, all models show the same main general features, namely a resistive continental crust under the Tepic-Zacoalco Rift (TZR) about 40 km thick, a series of conducting bodies in the SW half of the profile at depths above 30 km, and a dipping moderate conductor (~100 ohm-m) associated to the top of the oceanic subducting Rivera plate that dips at the same angle, apparently independent of rotation.

DISCUSSION OF RESISTIVITY MODELS

The interpretation of the projected and rotated to the regional strike resistivity model of profile MT-1 is presented in Figure 7, which in general shows a more conductive continental crust towards the trench. Conductive zones connecting with the surface can be associated to a combination of saturated fractures, upward fluid migration, and magma ascent feeding the volcanic front of central JB. The resistivity model depicts the subduction interface between the Rivera plate and the JB (red line), assumed to lie at the bottom of the elongated dipping conductor produced mainly by mineralized fluids. According to these results the altered crustal corner extents down to depths above ~30 km, within a distance of ~50 km onshore from the coast. In contrast to this broad conductive zone, the NE half of the profile model reveals a contrasting ~50–60 km thick resistive (>3 kOhm-m) continental crust overlain by a relatively thin (2–5 km) surface layer that associates with the conductive volcano-sedimentary infill of the Tepic-Zacoalco rift valley (TZR). The white dashed line in this section indicates the interpreted lower limit of the resistive continental crust that appears to be thinning towards the trench, where the continental crust seems intensely fractured, probably by a combination of subduction erosion and upwards migration of fluids.

The conductivity structure in the southwestern part of the profile obeys to fluids derived from low grade dehydration reactions mixed with saline fluids that permeated the rock matrix through micropores and fractures. Small percentages of interconnected saline fluids (1–5 %) have been shown to increase the electric conductivity by several orders of magnitude (Hyndman and Shearer, 1989), therefore the anomalous broad high conductivity zone (~10–50 Ohm-m) may be an indication of the electrical characteristics of the fluid as well as of the fracture pattern associated to the stress field at the active front. Although our lateral resolution is limited, the observed resistivity patches point out to a fragmented continental crust at the

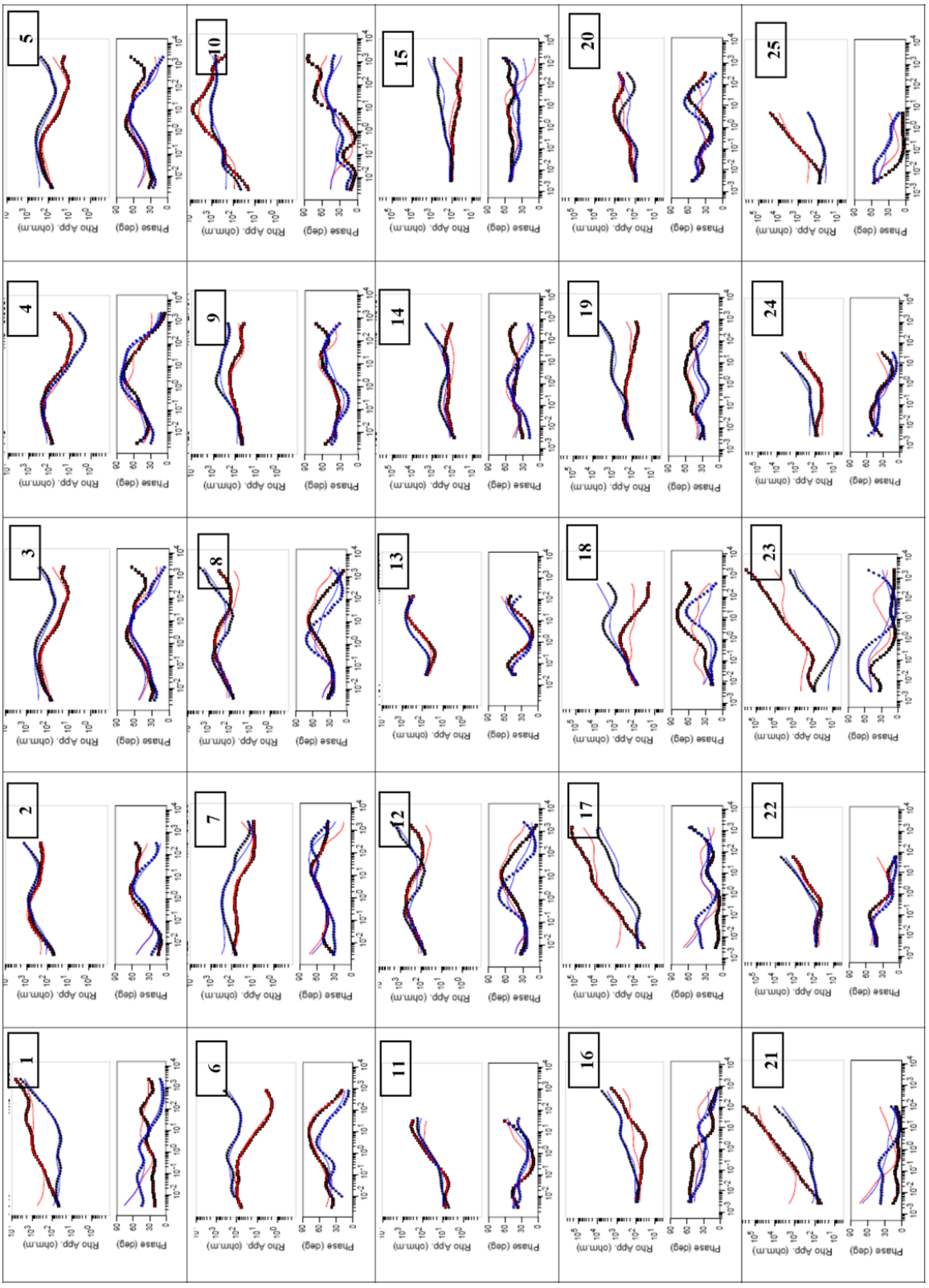

Figure 4. Plots of the resistivity and phase field curves rotated to the regional strike (N9W) for sites 1-13 of profile MT-1 and sites 14-25 of profile MT-3, obtained from the dimensionality analysis using the method of Caldwell *et al.* (2004), along with the fitting curves from the data inversion. Best misfit obtained for MT-1 was RMS =4.7 after 65 iterations and for MT-3 was RMS= 4.5 after 70 iterations.

subduction corner. Overpressure at the bending plate and low grade metamorphic reactions that release fluids through the breakdown of hydrated minerals (*e.g.*, smectites, micas and zeolites) at starting temperatures of ~150 ºC (Peacock, 1990; Marquis and Hyndman, 1992; Rüpke *et al.*, 2002) are thought to be responsible for the observed anomalous conductor; both crystal cleavage and interconnected fracture matrix are known to be efficient electric current promoters.

At depths between 40 and 60 km, and 25 to 75 km away the coast below the thinned crust, an extensive low resistivity (<100 Ohm-m) zone under the altered crust is interpreted as a mixture of metasomatic hydrous minerals and buoyant mantle materials above the unbended oceanic slab. Intense dewatering processes appear to occur in this depth interval by metamorphic reactions in the slab at intermediate P-T conditions. Jödicke *et al*. (2006) proposed that lawsonite-blueschist metamorphic reactions release considerable amounts of water at depths of ~40 km along the low angle subducting Cocos plate. Lawsonite breakdown alone is reported to have the potential to release 3.3 wt% water at ~450 °C and pressures above 1.6 GPa.

The P-T conditions at the subduction front and the dipping angle of the slab are closely related to convergence velocity, and appears to have an important influence on the distance of the volcanic front from the trench (Peacock and Wang, 1999). In the JB, low convergence rates (~20–33 mm/yr; Kostoglodov and Bandy, 1995) and a dip angle of the subducted slab >45° are consistent with these results. Slow convergence rate combined with a steep dipping slab shifts the mantle wedge isotherms upwards (Peacock and Wang, 1999), producing dehydration reactions at closer distances from the trench. Observed trenchward migration of magmatism (Ferrari *et al,*, 2001) provides evidence of a steepening of the subducted slab in this area, which is consistent with dehydration reactions closer to the trench at intermediate P-T conditions (~1.5 GPa, ~500 °C), occurring within shorter distances than in the neighboring Cocos plate (Ferrari *et al.*, 2012).

A remarkable feature of this region of the JB is the occurrence of lamprophyres along the volcanic front (Luhr

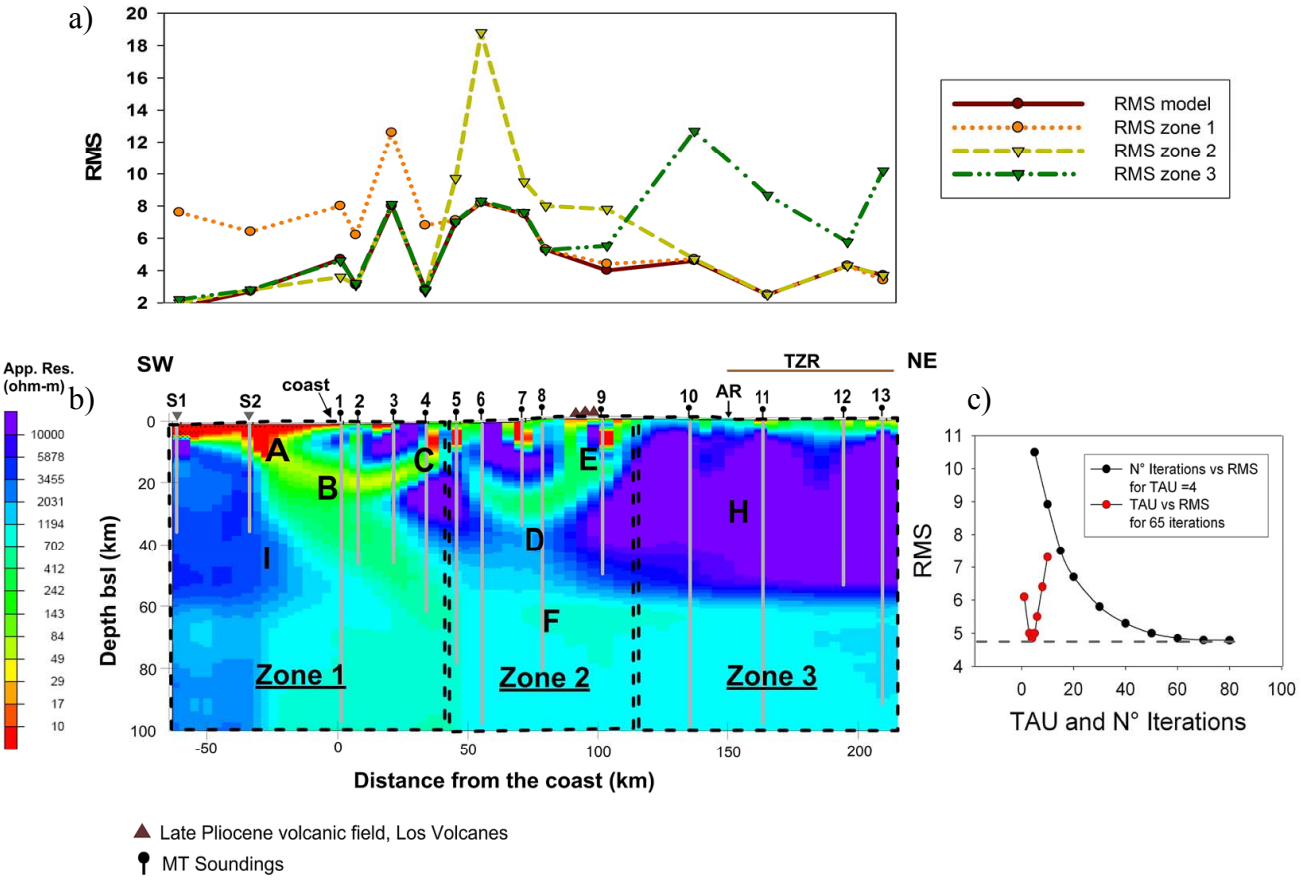

Figure 5. Resistivity model of MT-1 profile obtained after 65 iterations using the optimal regularization parameter τ = 4 (see RMS *vs.* TAU plot to the lower right). The mean quadratic error associated with the model fit was RMS=4.7. In order to test if the resulting anomalous conductive zones were required by the data, such conductors were replaced with a background crustal resistivity (2000 ohm-m) once at a time. The upper part of the figure shows the graph of the RMS errors obtained when replacing the conductors A, B, and C in zone 1 (dotted line), then the conductors D, E, and F in zone 2 (dashed line), and finally the conductor below resistive feature H in zone 3 (dotted-dashed line), respectively. The RMS error increases considerably when the conductors are absent. The investigation depths along the profile (vertical grey lines bellow MT stations) were estimated using the Niblett-Bostick approximation that uses the average conductance of a layered earth. Abreviations are as follows: TZR=Tepic-Zacoalco rift; AR = Ameca river.

et al., 2006). Within the JB, the northern part of the Los Volcanes-Atenguillo volcanic field is formed by alkaline intraplate-type volcanic rocks, whereas the volcanic fields along the CJVL are formed by calc-alkaline rocks and a roughly equal proportion of K_2O-rich lamprophyric rocks (minettes, hornblende-lamprophyres, absarokites, and spessartites). Lamprophyres are igneous rocks characterized by the presence of hydrous minerales like phlogopite and/or hornblende and the absence of plagioclase phenocrysts (Gómez-Tuena *et al.*, 2011), which crystallize from K_2O-rich magmas with high water contents. Gómez-Tuena *et al.* (2011) interpreted that the compositional variability of magmatism in western Mexico is related to the addition to the mantle wedge of different subduction agents, presumably extracted from the slab at different metamorphic stages, leading to the formation of calc-alkaline and high-K_2O volcanic rocks. The chemical character of the metamorphic minerals and fluids is similar to that recognized in arcs with a well-defined K_2O to slab depth (K-*h*) relationship, but the variations in the Rivera plate subduction zone occur in a margin that is much narrower than in other arcs because of the steeper subduction. Hydrous minerals in a mantle

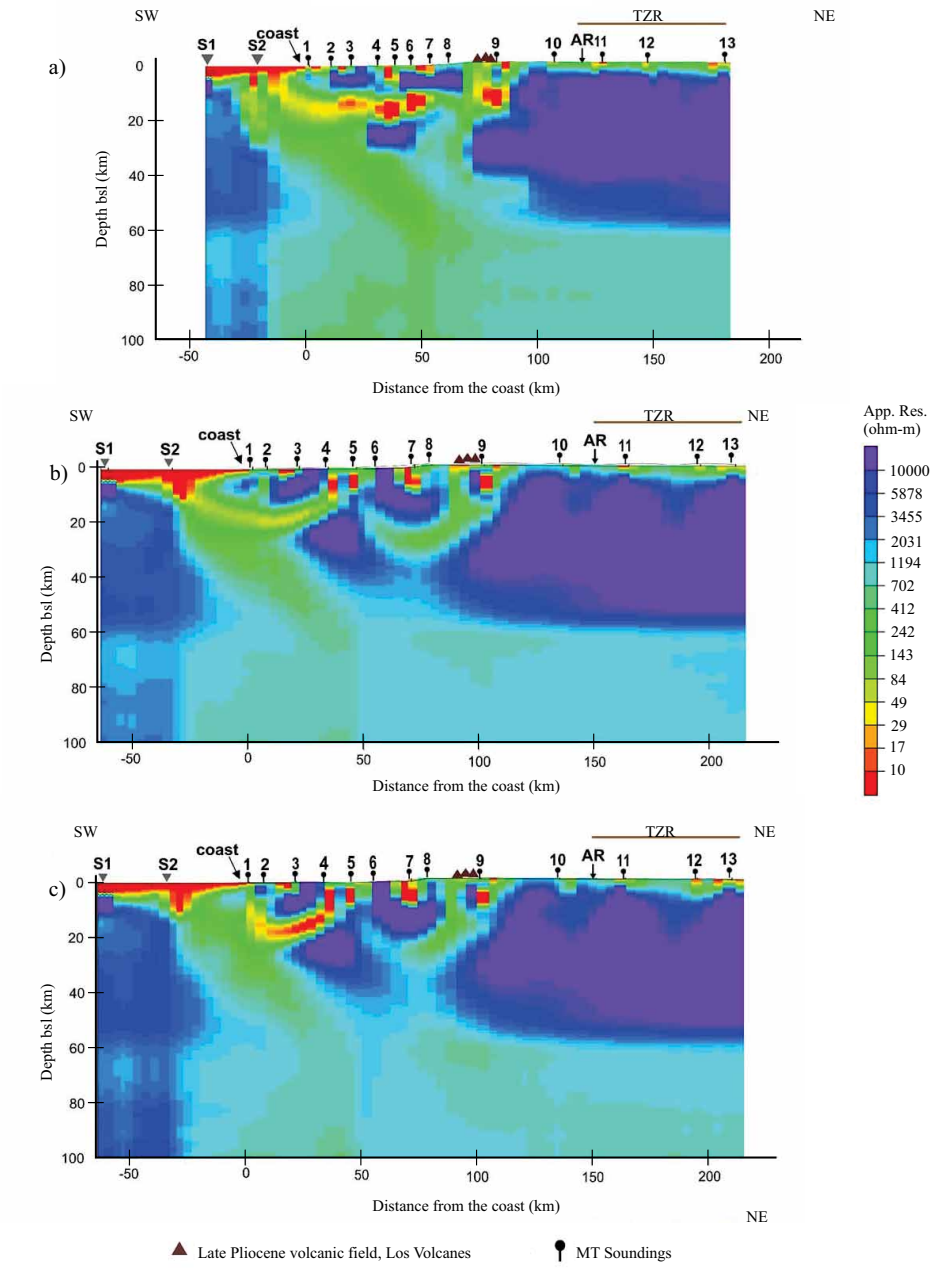

Figure 6. Resistivity models for profile MT-1 using the same parameters for inversion. a: Soundings rotated to the regional strike (N9W) and projected along a profile perpendicular to the MT transect; b: the inverted polarity model; and c: rotated to the principal axis (Swift, 1967) model. Generally speaking, the three resistivity images show the same enhanced conductivity zones and resistive features. TZR: Tepic-Zacoalco rift; AR: Ameca river.

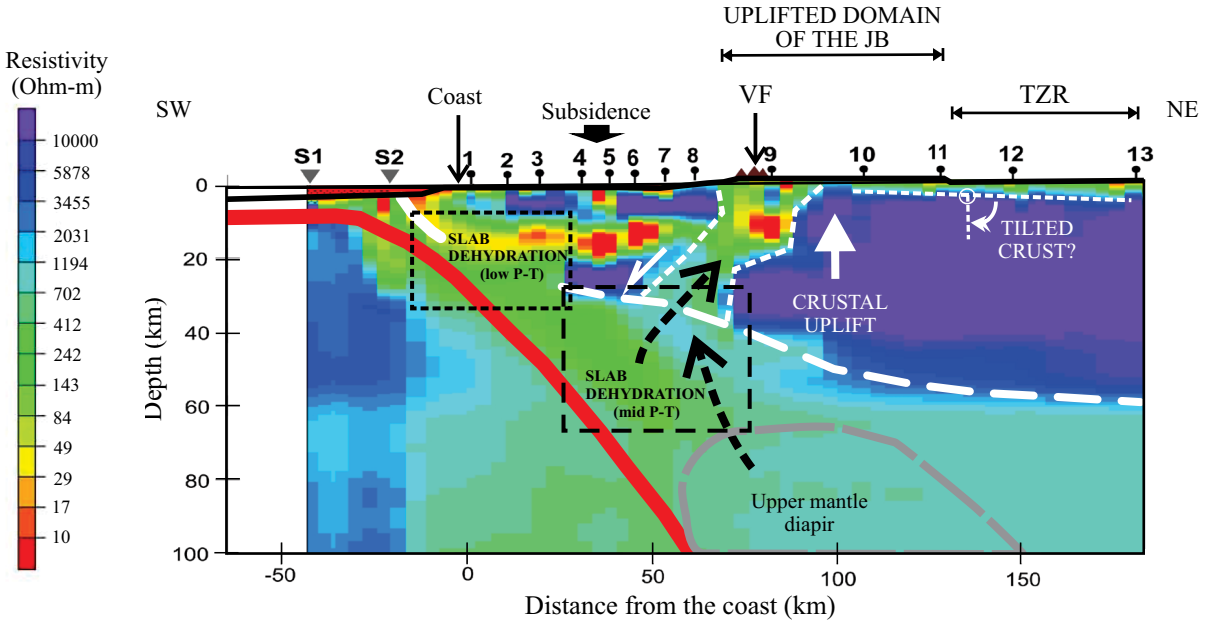

Figure 7. Interpretation of the rotated to the regional strike (N9W) and projected MT resistivity model along the MT-1 profile located in the central Jalisco block. Upper crustal anomalous conductors at the convergence front are interpreted as fractured zones permeated by mineralized conducting fluids, and partial melts below the volcanic front (VF). The oceanic slab-continental crustal interface is assessed from the diffuse conductive dipping signature assumed to lie on top of the subducting slab (continuous red line). Buoyant upper mantle material mixed with mantle zones metasomatized by fluids released from moderate P-T metamorphic reactions in the subducted slab (~60 km) uplift and tilt the fragile upper crust inducing thinning and weakening that promote faulting at the convergence front of the NA and Rivera plates. Much of the shallow seismicity above 20–30 km must be responding to fluid and partial melt migration along the fractured zones. TZR: Tepic-Zacoalco rift.

wedge metasomatized by subduction agents are more easily melted, and tapped to produce magmas with high water content that may ascend during extensional episodes through a weakened crust. In this scheme, the moderately conductive mantle plume drags hydrous minerals upwards from depths >80 km above the slab (Figure 7) into the melting zone. Also, intraplate-type magmas can originate by decompression melting related to diapiric upwelling of upper mantle material (Figure 7) negligibly modified by subduction agents. This evidence is consistent with the existence of a fragmented upper crust that allows the ascent of magmas and fluids. The dashed arrows in the resistivity images of Figure 7 indicate conductivity paths associated to migrating mineralized fluids and melts in the weakened crust. Besides, we postulate that the weakened crust and the buoyancy of upwelling hydrated mantle material induce uplift and consequent faulting of a sector of the Jalisco block.

León-Soto *et al*. (2009) deduced that asthenospheric mantle material rises through a gap between the subducted Cocos and Rivera plates, inducing a toroidal flow in this area at a short distance from the trench. The infiltration of hot and buoyant asthenospheric mantle would have promoted slab steepening (Yang *et al.*, 2009). These seismic derived models are consistent with the steeply subducting slab model of the MT-1 profile, where in addition an eroded and uplifted continental crust can be explained by the predicted mantle flow from the gap between the Rivera and Cocos slabs. The existence of mantle materials in the corner front of the subduction system is consistent with the relative abundance of mantle derived He in thermal waters (Taran *et al*., 2002) and magmas around the JB.

According to Kostoglodov and Bandy (1995) the maximum seismic length projected horizontally as well as the maximum depth of seismicity in the JB, both diminish westwards and wedge towards the Bahía de Banderas fault zone, suggesting that the subduction angle of the subducted Rivera plate varies rapidly along the JB, with increasing dip toward the northwest. This is supported by the conductivity images of the modeled profiles MT-1 and MT-3 regardless if we use principal axis or rotated to the strike models (Figure 8). The slab dip at ~60 km depth estimated from the model profile MT-1 is ~50° whereas that from model profile MT-3 is ~65°, a difference of 15° in a distance of about 50 km. Comparison of Yang *et al.* (2009) and Gorbatov and Fukao (2005) seismic tomographic P-wave velocity models confirm a steeper subduction towards the NW of the JB. Yang *et al.* (2009) tomography section A1-B1 is coincident with our resistivity image MT-1, however at crustal depths <60 km our model match better with the hypocenters of local seismicity than the P wave tomography model. The slab dip in the tomography model of Gorbatov and Fukao (2005) is similar to that in our MT-3 resistivity profile, which passes to the southwest of their transect C-C´. Their velocity image along the segment coincident with our profile (nearly 200 km) is consistent with the results along the MT section in that both predict a steeper dip angle for the top of the oce-

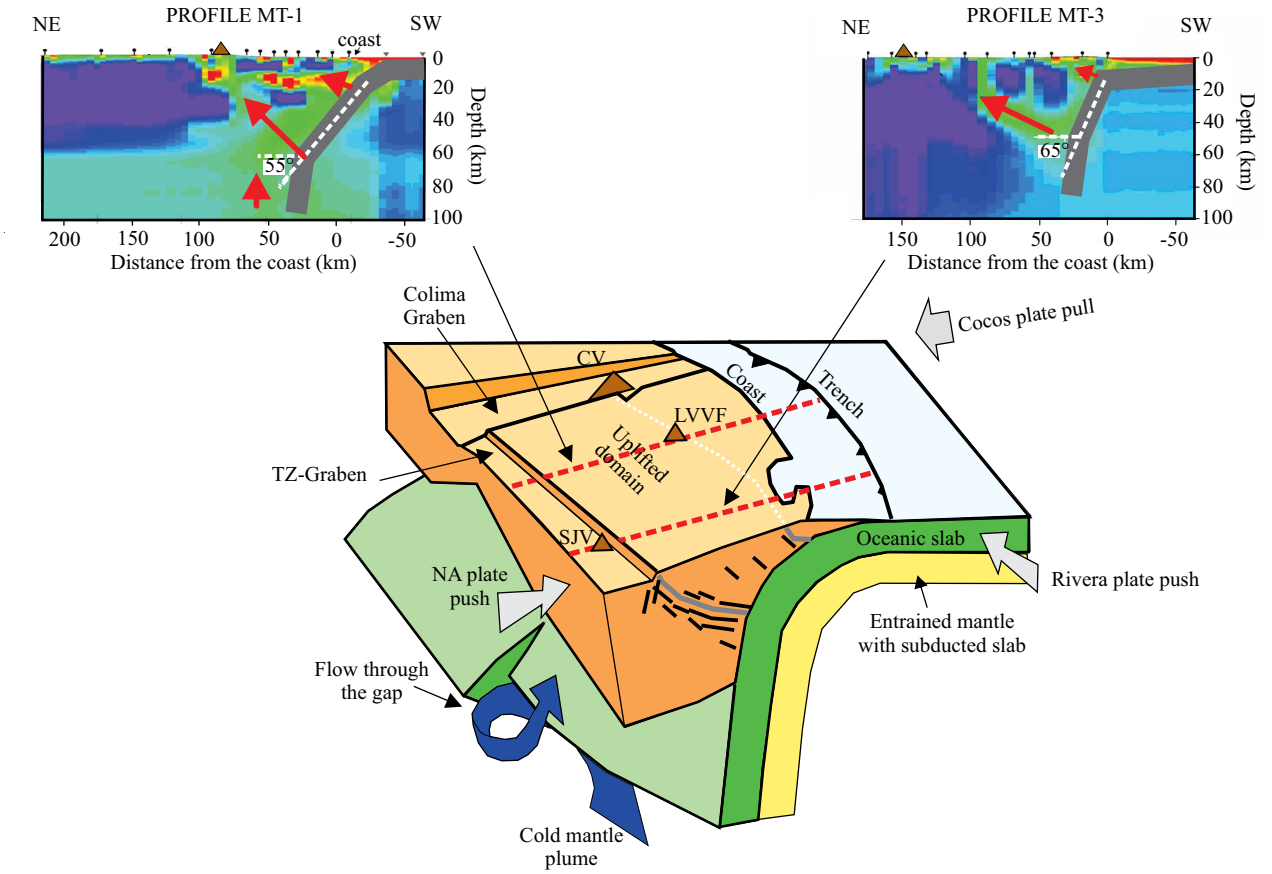

Figure 8. Cartoon view of the Rivera plate facing southwards (modified after León-Soto *el al.*, 2009) using the resistivity images of the MT-1 and MT-3 profiles. Dip angle of the subducting slab is ~50° along MT-1 whereas along the MT-3 model is about 65°, *i.e.*, a difference of 15° in a distance of about 50 km. Red arrows in the models suggest conductivity paths associated to migration of mineralized fluids. A steeper slab dip and thicker crust is interpreted in the area of the Bahía de Banderas fault zone while to the southeast of the JB the slab dip angle decreases toward the gap between the Rivera and Cocos plates. The resistivity image of profile MT-1 is consistent with a buoyant mantle plume. CV: Colima volcano; LVVF: Los Volcanes volcanic field SJV San Juan volcano; TZ: Tepic-Zacoalco.

anic crust at the NW corner of the Jalisco block. Results of numerical modeling by Cailleau and Oncken (2008) indicate that, regardless of the distribution of friction planes along the interface between the continental crust and oceanic subducting slab, there is at least one thrust fault rooting at the subduction interface and emerging toward the surface of the ground associated to volcanism. Their modeling also predicts subsidence in the fore arc zone always preceding uplift of the continental crust as is observed in the interpreted MT-1 section. The resistive continental crust may be as well tilted as suggested by our model results (Figure 7).

CONCLUSIONS

We have imaged the electrical conductivity distribution along two magnetotelluric transects, which provide insights into the Rivera Plate subducting geometry at depths above ~60 km at the northwestern corner of the Jalisco block. The enhanced conductivity zones along the two MT profiles unveil structural aspects at the convergence front of the Rivera and North American plates, which were previously unknown or only suspected. The orientations of the phase impedance polarization ellipses as well as independent determinations of the regional strike have nearly coincident directions with the convergence velocity field within the Rivera plate (Kostoglodov and Bandy, 1995) that describe its relative motion with respect to NA. Electric (strike and ellipses) and orthogonal magnetic field derived induction vectors are also consistent with trench normal, fast SKS directions associated to a two dimensional ~NNE mantle anisotropy in the central part of the JB (León-Soto *et al.*, 2009); however, observed inconsistent induction vector directions at the NW end of the JB suggest a change in the electrical imprint of surrounding mantle, probably responding to a rapid change in the subduction regime.

ACKNOWLEDGEMENTS

This work was funded by projects PAPIIT-UNAM IN115608, IN120509-1 and IN120509-2, and CONACyT

PA7078-F. The observations and commentaries of the reviewers have been of great value to improve the original manuscript. We acknowledge the support of Lenin Ávila, Héctor La Madrid, and Ienisei Peña during the acquisition field campaigns.

REFERENCES

Allan, J.F., 1986, Geology of the northern Colima and Zacoalco grabens, southwest Mexico: Late Cenozoic rifting in the Mexican Volcanic Belt: Geological Society of America Bulletin, 97, 473-485.

Allan, J.F., Nelson, S.A., Luhr, J.F., Carmichael, I.S.E., Wopat, M., Wallace, P.J., 1991, Pliocene-Holocene rifting and associated volcanism in southwest Mexico: An exotic terrane in the making, *in* Dauphin J.P., Simoneit B.R.T. (eds.), The Gulf and Peninsular Province of the Californias: American Association of Petroleum Geologists, Memoir 47, 425-445.

Alvarez, R., 2002, Banderas Rift Zone: A plausible NW limit of the Jalisco Block: Geophysical Research Letters 29 (20), art. No. 1994, Oct. 15, (doi:10.1029/2002GL016089).

Alvarez, R., López-Loera, H., Arzate, J., 2006, Evidence of the existence of an uplifted and a static domain in the Jalisco Block, *in* Backbone of the Americas: Patagonia to Alaska, Mendoza, Argentina: Geological Society of America, Abstracts with Programs, Specialty Meetings No. 2, p.108.

Arzate, J.A., Mareschal, M., Livelybrooks, D., 1995, Electrical image of the subducting Cocos Plate from magnetotelluric observations: Geology, 23(8), 703-706.

Arzate, J.A., Álvarez, R., Yutsis, V., Pacheco, J., López-Loera, H., 2006, Geophysical modeling of valle de Banderas graben and its structural relation to Bahía de Banderas, Mexico: Revista Mexicana de Ciencias Geológicas, v.23, 2, 184-198.

Atwater, T., Stock, J., 1998, Pacific-North America plate tectonics of the Neogene Southwestern United States: An update: International Geology Review, 40(5), 375-402.

Bahr, K., 1988, Interpretation of the magnetotelluric impedance tensor: regional induction and local telluric distortion: Jounal of Geophysics, 62, 119-127.

Bahr, K., 1991, Geological noise in magnetotelluric data: a classification of distortion types: Physics of the Earth and Planetary Interiors, 66, 24-38.

Bandy, W., Mortera-Gutiérrez, C., Urrutia-Fucugauchi, J., Hilde, T.W.C., 1995, The subducted Rivera-Cocos plate boundary: Where is it, what is it, and what is its relationship to the Colima rift?: Geophyscal Reseacrh Letters, 22, 3075-3078.

Bandy, W.L., Urrutia-Fucugauchi, J., McDowell, F.W., Morton-Bermea O., 2001, K-Ar ages of four mafic lavas from the Central Jalisco Volcanic Lineament: supporting evidence for a NW migration of volcanism within the Jalisco Block, western Mexico: Geofísica Internacional, 40, 259-269.

Bostick, F.X., 1977, A simple almost exact method of magnetotelluric analysis, *in* Ward, S. (ed.), Workshop of Electrical Methods in Geothermal Exploration: University of Utah, Research Institute, U.S. Geological Survey.

Bourgois, J., Renard, V., Aubouin, J., Bandy, W., Barrier, E., Calmus, T., Carfantan, J., Guerrero, C., Mammerickx, J., Mercier de Lepinay, B., Michaud, F., Sosson, M., 1988, Active fragmentation of the North American plate: offshore boundary of the Jalisco block off Manzanillo: Comptes Rendues, Académie des Sciences Paris, t. 307,Serie II, 1121-1130.

Brasse, H., Laezaeta, P., Rath, V., Schwalenberg, K., Soyer, W., Haak, V., 2002, The Bolivian Altiplano conductivity anomaly: Journal of Geophysical Research, 107, doi:10.1029/2001JB000391.

Brasse, H., Kapinos, G., Mütschard, L., Alvarado, G.E., Worzewski, T., Jegen, M., 2008, Deep electrical resistivity structure of northwestern Costa Rica: Geophysical Research Letters, 36, L02310 doi:10.1029/2008GL036397.

Brown, H.E., 2007, Structure of the Rivera plate beneath the Jalisco block, western Mexico: USA, University of Wyoming, Ph.D. thesis.

Caldwell, T.G., Bibby, H.M., Brown, C., 2004, The magnetotelluric phase tensor: Geophysical Journal International, 158, 457-469.

Cailleau B., Oncken, O., 2008, Past forearc deformation in Nicaragua and coupling at the megathrust interface: Evidence for subduction retreat?: Geochemistry, Geophysics, and Geosystems (G3), doi:10.1029/2007GC001754.

Calmus, T., Poupeau, G., Mercier de Lepinay, B., Michaud, F., Burgois, J., 1995, Apatite fision-track ages of plutonic rocks sampled along the active margin off Manzanillo and in the Puerto Vallarta batholith, Mexico: Geos (Boletín Unión Geofísica Mexicana), 15(2), 63-64.

DeMets, C., Traylen, S., 2000, Motion of the Rivera plate since 10 Ma relative to the Pacific and North American plates and the mantle: Tectonophysics, 318, 119-159.

Durham, J.W., Applegate, S.P., Espinosa-Arrubarena L., 1981, Onshore marine Cenozoic along southwest Pacific coast of Mexico: Geological Society of America Bulletin, 92, 384-394.

Ferrari, L., 1995, Miocene shearing along the northern boundary of the Jalisco block and the opening of the southern Gulf of California: Geology, 23, 751-754.

Ferrari, L., Pasquare, G., Venegas, S., Castillo, D., Romero F., 1994, Regional tectonics of western Mexico and its implications for the northern boundary of the Jalisco block: Geofísica Internacional, 33(1), 139-151.

Ferrari, L., Pasquarè, G., Venegas-Salgado S., Romero-Ríos F., 2000, Geology of the western Mexican Volcanic Belt and adjacent Sierra Madre Occidental and Jalisco Block: Geological Society of America Special Paper, 334, 65-83.

Ferrari, L., Petrone, Ch., Francalanci, L., 2001, Generation of oceanic-island basalt–type volcanism in the western Trans-Mexican volcanic belt by slab rollback, asthenosphere infiltration, and variable flux melting: Geology, 29, 507-510.

Ferrari, L., Orozco-Esquivel, T., Manea, V., Manea, M., 2012, The dynamic history of the Trans-Mexican Volcanic Belt and the Mexico subduction zone: Tectonophysics, 522-523, 122-149.

Garduño-Monroy, V.H., Saucedo-Girón, R., Jiménez, Z., Gavilanes-Ruiz, J.C., Cortés-Cortés, A., Uribe-Cifuentes, R.M., 1998, La Falla Tamazula, límite suroriental del Bloque de Jalisco y sus relaciones con el complejo volcánico de Colima, México: Revista Mexicana de Ciencias Geológicas, 15, 2, 132-144.

Gorbatov, A., Fukao, Y., 2005, Tomographic search for missing link between the ancient Farallon subduction and the present Cocos subduction: Geophysical Journal International, 160, 849-854.

Gómez-Tuena, A., Orozco-Esquivel, M., Ferrari, L., 2007, Igneous petrogenesis of the Transmexican Volcanic Belt, *in* Alaniz-Álvarez, S.A., Nieto- Samaniego, A.F. (eds.), Geology of México: Celebrating the Centenary of the Geological Society of México: Geological Society of America Special Paper 422, 129-181.

Gómez-Tuena, A., Mori, L., Goldstein, S., Pérez-Arvizu, O., 2011, Magmatic diversity of western Mexico as a function of metamorphic transformations in the subducted oceanic plate: Geochimica et Cosmochimica, Acta 75, pp 213–241.

Groom R.W., Bailey R.C., 1989, Decomposition of magnetotelluric impedance tensor in the presence of local three-dimensional galvanic distortion: Journal of Geophysical Research, 94, 1913-1925.

Hyndman, R.D., 1988, Dipping seismic reflectors, electrically conductive zones and trapped water in the crust over a subducting plate: Journal of Geophysical Research, 93, 13391-13405.

Hyndman, R.D., Shearer, P.M., 1989, Water in the lower continental crust: modelling magnetotelluric and seismic reflection results: Geophysical Journal International, 98, 343-365.

Jödicke, H., Jording A., Ferrari L., Arzate J., Mezger K., Rüpke L., 2006, Fluid release from the subducted Cocos plate and partial melting of the crust deduced from magnetotelluric studies in southern Mexico: Implications for the generation of volcanism and subduction dynamics: Journal Geophysical Research, 111, B08102, doi:10.1029/2005JB003739.

Johnson C.A., Harrison, C.G.A., 1990, Neotectonics in central Mexico:

Physics of the Earth and Planetary Interiors, 64, 187-210.
Jones, A.G., 1983, The problem of current channelling. A critical review: Geophysical Surveys, 6, 79-122.
Jording, A., Ferrari, L., Arzate, J.A., Jödicke, H., 2000, Crustal variations and terrane boundaries in southern Mexico as imaged by magnetotelluric transfer functions: Tectonophysics, 327, 1-13.
Klitgord, K., Mammerickx, J., 1982, East Pacific rise: Magnetic anomaly and bathymetric framework: Journal of Geophysical Research, 87, 6725-6750.
Kostoglodov, V., Bandy, W., 1995, Seismotectonic constraints on the convergence rate between the Rivera and North American plates: Journal of Geophysical Research, 100, B9, 17977-17989.
Kurtz, R.D., Delaurie, J.M., Gupta, J.C., 1986, A magnetotelluric sounding across Vancouver Island sees the subducting Juan de Fuca plate: Nature, 312, 596-599.
Kurtz, R.D., Delaurie, J.M., Gupta, J.C., 1990, The electrical conductivity distribution beneath Vancouver Island: A region of active plate subduction: Journal of Geophysical Research, 95, 10929-10946.
León-Soto, G., Ni, J.F., Grand, S.P., Sandvol, E., Valenzuela, R.W., Guzmán-Speziale, M., González-Gómez J.M., Domínguez-Reyes, T., 2009, Mantle flow in the Rivera-Cocos subduction zone: Geophysical Journal International, 179, 1004-1012.
Luhr, J. F., 1997, Extensional tectonics and the diverse primitive volcanic rocks in the western Mexican Volcanic Belt: The Canadian Mineralogist, 35, 473-500.
Luhr, J.F., Nelson, S.A., Allan, J.F., Carmichael, I.S.E., 1985, Active rifting in southwest Mexico: Manifestations of an incipient eastward spreading ridge jump: Geology, 13, 54-57.
Luhr, J. F., Kimberly, P., Siebert, L., Aranda-Gómez, J.J., Housh, T.B., Kysar, G., 2006, México's Quaternary volcanic rocks: Insights from the MEXPET petrological and geochemical database: Geological Society of America Special Paper 402, 1-44.
Maillol, J.M., Bandy, W.L., Ortega-Ramírez, J., 1997, Paleomagnetism of Plio-Quaternary basalts in the interior of the Jalisco Block, western Mexico: Geofísica Internacional, 36, 21-35, 1997.
Marquis, O., Hyndman, R.D., 1992, Geophysical support for aqueous fluids in the deep crust-seismic and electrical relationships: Geophysical Journal International 110, 91-105.
Martí, A., Queralt, P., Roca, E., 2004, Geoelectric dimensionality in complex geological areas: application to the Spanish Betic Chain: Geophysical Journal International, 157, 961-974.
Mercier de Lépinay, B., Michaud, F., Calmus, T., Bourgois, J., Poupeau, G., Saint-Marc, P., Bandy, W., Castrec, M., Guerrero-García, J., Sosson, M., Villeneuve, M., Rinaldi, C., 1997, Large Neogene subsidence event along the Middle America Trench off Mexico (18°N-19°N): Evidence from submersible observations: Geology, 25, 5, 387-390.
Niblett, E.R., Sayn-Wittgenstein, C., 1960, Variation of the electrical conductivity with depth by the magnetotelluric method: Geophysics, 25, 998-1008.
Núñez-Cornú, F., Rutz, M.L., Nava, F.A., Reyes-Dávila, G., Suárez-Plascencia, C., 2002, Characteristics of seismicity in the coast and north of Jalisco Block, Mexico: Physics of the Earth and Planetary Interior, 132, 141-155.
Peacock, S.M., 1990, Fluid processes in subduction zones: Science, 248, 329-337.
Peacock, S.M., Wang, K., 1999, Seismic consequences of warm versus cool subduction metamorphism: Examples from southwest and northeast Japan: Science, 286, 937-939.
Ramírez-Herrera, M.T., Kostoglodov, V., Urrutia-Fucugauchi, J., 2004, Holocene-emerged notches and tectonic uplift along the Jalisco coast, Southwest Mexico: Geomorphology, 58, 291-304.
Righter, K., Rosas-Elguera, J., 2001, Alkaline lavas in the volcanic front of the Western Mexican Volcanic Belt: Geology and petrology of the Ayutla and Tapalpa volcanic fields: Journal of Petrology, 42(12), 2333-2361.
Righter, K., Carmichael, I.S.E., 1992, Hawaiites and related lavas in the Atenguillo graben, western Mexican Volcanic Belt: Geological Society of America Bulletin, 104, 1592-1607.
Rodi, W.L., Mackie, R.L., 2001, Nonlinear conjugate gradients algorithm for 2-D magnetotelluric inversion: Geophysics, 66, 174-187.
Rosas-Elguera, J., Ferrari, L., Garduño-Monroy, V.H., Urrutia-Fucugauchi, L., 1996, Continental boundaries of the Jalisco block and their influence in the Pliocene-Quaternary kinematics of western Mexico: Geology, 24, 921-924.
Rüpke, L.H., Phipps-Morgan, J., Hort, M., Connolly, J.A.D., 2002, Are the regional variations in Central American arc lavas due to differing basaltic versus peridotitic slab sources of fluids?: Geology, 30, 1035-1038.
Schaaf, P., Morán-Zenteno, D., Hernández-Bernal, M.S., Solís-Pichardo, G., Tolson, G., Köhler, H., 1995, Paleogene continental margin truncation in southwestern Mexico: Geochronological evidence: Tectonics, 14, 1339-1350.
Schwarz, G., Krüger, D., 1997, Resistivity cross section through the Southern Central Andean crust as inferred from 2-D modelling of magnetotelluric and geomagnetic deep sounding measurements: Journal of Geophysical Research, 102, B6, 11957-11978.
Simpson, F., Bahr, K., 2005, Practical magnetotellurics: Cambridge University Press, 254 pp.
Soyer, W., Unsworth, M.J., 2006, Deep electrical structure of the northern Cascadia subduction zone (British Columbia, Canada): implications for the role of fluids: Geology, 34, 1, 53-56.
Swift, C.M., 1967, A magnetotelluric investigation of an electrical conductivity anomaly Southwestern United States: Cambridge Massachusetts Institute of Technology, Ph.D. thesis.
Taran, Y., Inguaggiato, S., Varley, N., Capasso, G., Favara, R., 2002, Helium and carbon isotopes in thermal waters of the Jalisco block, Mexico: Geofísica Internacional, 41(4), 459-466.
Waff, H.S., Rygh, J.T., Livelybrooks, D.W., Clingman, W.W., 1988, Results of a magnetotelluric transverse across western Oregon: crustal resistivity structure and the subduction of the Juan de Fuca plate: Earth and Planetary Science Letters, 87, 313-324.
Wannamaker, P.E., Booker, J.R., Jones, A.G., Chave, A.D., Filloux, J.H., Waff, H.S., Law, L.K., 1989, Resistivity cross section through the Juan de Fuca subduction system and its tectonic implications: Journal of Geophysical Research, 94, 14127-14144.
Weaver, J.T., Agarwal, A.K., Lilley, F.E.M., 2000, Characterisation of the magnetotelluric tensor in terms of its invariants: Geophysical Journal International, 141, 321-336.
Wight, D., Bostick, F., 1980, Cascade decimation –A technique for real time estimation of power spectra, *in* Acoustics, Speech, and Signal Processing, IEEE International Conference on ICASSP'80, 5, 626- 629.
Yang, T., Grand, S.P., Wilson, D., Guzmán-Speziale, M., Gómez-González, J.M., Domínguez-Reyes, T., Ni, J., 2009, Seismic structure beneath the Rivera subduction zone from finite-frequency seismic tomography: Journal of Geophysical Research, 114, B01302, doi:10.1029/2008JB005830.

Manuscript received: January 8, 2013
Corrected manuscript received: Mach 27, 2013
Manuscript accepted: April 6, 1013